

Published in final edited form as:

*Neuron*. 2011 June 9; 70(5): 847–854. doi:10.1016/j.neuron.2011.04.001.

## Synaptophysin regulates the kinetics of synaptic vesicle endocytosis in central neurons

Sung E. Kwon and Edwin R. Chapman\*

Howard Hughes Medical Institute and Department of Neuroscience, University of Wisconsin, Madison, Wisconsin 53706

### Summary

Despite being the most abundant synaptic vesicle membrane protein, the function of synaptophysin remains enigmatic. For example, synaptic transmission was reported to be completely normal in synaptophysin knockout mice; however, direct experiments to monitor the synaptic vesicle cycle have not been carried out. Here, using optical imaging and electrophysiological experiments, we demonstrate that synaptophysin is required for kinetically efficient endocytosis of synaptic vesicles in cultured hippocampal neurons. Truncation analysis revealed that distinct structural elements of synaptophysin differentially regulate vesicle retrieval during and after stimulation. Thus, synaptophysin regulates at least two phases of endocytosis to ensure vesicle availability during and after sustained neuronal activity.

### Introduction

Synaptophysin (syp) was the first synaptic vesicle (SV) protein to be cloned and characterized (Jahn et al., 1985; Navone et al., 1986; Wiedenmann and Franke, 1985), and is now known to belong to a family of proteins with four transmembrane domains that includes synaptogyrin (syg) and synaptoporin (Sudhof et al., 1987). Syp is the most abundant SV protein by mass, accounting for ~10 % of total vesicle protein (Takamori et al., 2006). Each SV harbors ~32 copies of syp, which is second only to synaptobrevin (8% of the total SV protein) at ~70 copies per vesicle. Because syp is exclusively localized to SVs, it is widely used as a marker for pre-synaptic terminals.

Structurally, syp spans the vesicle membrane four times with a short amino- and a long carboxy-terminal tail, both of which are exposed on the cytoplasmic surface of the SV membrane. In addition, there are two short intravesicular loops that contain disulfide bonds. Syp is N-glycosylated on the first intravesicular loop and is phosphorylated on the long cytoplasmic tail; the function of these post-translational modifications remain unknown (Evans and Cousin, 2005; Pang et al., 1988; Wiedenmann and Franke, 1985). There is evidence suggesting that syp, especially its four transmembrane domains, may promote formation of highly curved membranes as in small SVs (Leube, 1995). Indeed, ectopic expression of syp alone in non-neuronal cells leads to formation of small cytoplasmic vesicles (Leube et al., 1989). A recent electron microscopy study revealed that syp forms hexameric structures that are similar to connexons (Arthur and Stowell, 2007).

© 2011 Elsevier Inc. All rights reserved.

\*To whom correspondence should be addressed: chapman@physiology.wisc.edu.

**Publisher's Disclaimer:** This is a PDF file of an unedited manuscript that has been accepted for publication. As a service to our customers we are providing this early version of the manuscript. The manuscript will undergo copyediting, typesetting, and review of the resulting proof before it is published in its final citable form. Please note that during the production process errors may be discovered which could affect the content, and all legal disclaimers that apply to the journal pertain.

Previous molecular studies have hinted at a number of diverse roles for *syp* in synaptic function including exocytosis, synapse formation, biogenesis and endocytosis of SVs (Cameron et al., 1991; Eshkind and Leube, 1995; Leube et al., 1989; Spiwox-Becker et al., 2001; Tarsa and Goda, 2002; Thiele et al., 2000; Thomas et al., 1988). Surprisingly, mice lacking *syp* were viable and had no overt phenotype (Evans and Cousin, 2005; McMahon et al., 1996). Synaptic transmission, and the morphology or shape of SVs, were not altered in *syp* knockout (*syp*<sup>-/-</sup>) mice (Eshkind and Leube, 1995; McMahon et al., 1996). The lack of an obvious phenotype was attributed to redundant expression of *syp* isoforms such as synaptogyrin (*syg*) or synaptoporin. Consistent with this notion, mice lacking both *syp* and *syg* exhibited diminished long-term potentiation (Janz et al., 1999). Nevertheless, recent genetic screening in human subjects, and behavioral studies in mice, have implicated loss or truncation of *syp* in mental retardation and/or learning deficits (Schmitt et al., 2009; Tarpey et al., 2009). These new results suggest that *syp* might play a subtle yet important role in regulating synaptic transmission in neuronal circuits involved in learning and memory.

As alluded to above, it is not clear as to whether *syp* functions in the SV recycling pathway in central neurons. To test this notion directly, we performed a quantitative analysis of SV recycling in cultured neurons using optical and electrophysiological methods. We show that *syp* regulates the endocytosis of SVs both during and after sustained neuronal activity via distinct structural determinants. We further show that the observed defects in endocytosis, due to loss of *syp*, exacerbate synaptic depression and delay the replenishment of releasable SV pools.

## Results

### Synaptophysin regulates the kinetics of compensatory SV endocytosis

To determine whether *syp* functions in the SV recycling pathway, we directly monitored the trafficking of SV proteins tagged with the pH-sensitive GFP, pHluorin (Miesenbock et al., 1998; Sankaranarayanan and Ryan, 2000), in dissociated hippocampal neurons from *syp* knockout (*syp*<sup>-/-</sup>) mice. We used two different optical reporters, *syt1*-pH and *SV2A*-pH, in which a pHluorin was fused to the intra-luminal domain of the SV membrane protein synaptotagmin 1 (*syt1*) or *SV2A*, respectively (Fernandez-Alfonso et al., 2006). These reporters were expressed in neurons using lenti-virus. *SV2A*-pH is a novel reporter; its use in monitoring the SV cycle in cultured neurons was validated as shown in Fig. S1. In short, *SV2A*-pH is efficiently targeted to recycling SVs and its expression does not interfere with the normal SV recycling pathway (Fig. S1, A–D).

We compared the kinetics of SV endocytosis following sustained stimulation in wild-type (wt) and *syp*<sup>-/-</sup> neurons. At rest, the fluorescence of *syt1*-pH remained quenched due to the low pH of the vesicle lumen (pH 5.5) (Fig. 1C). Exocytosis, evoked by delivering 300 stimuli (10 Hz), led to a rapid rise in fluorescence due to dequenching of the pHluorin signal upon exposure to the slightly alkaline extracellular solution (pH 7.4), followed by a slow decay due to subsequent endocytosis and re-acidification of vesicles (Fig. 1, A and C). Average time constants ( $\tau$ ) of the post-stimulus fluorescence decay were significantly greater in *syp*<sup>-/-</sup> versus wt neurons ( $\tau = 18.6 \pm 1.8$  s for wt,  $\tau = 29.6 \pm 1.5$  s for *syp*<sup>-/-</sup>) (Fig. 1, A and F), indicating slower SV endocytosis and/or re-acidification. To distinguish between these possibilities, we measured the time-course of vesicle re-acidification and found that the rates were identical in wt ( $\tau = 3.13 \pm 1.2$  s) versus *syp*<sup>-/-</sup> neurons ( $\tau = 3.31 \pm 1.2$  s) (Fig. S1E); these time constants are in agreement with previous studies using cultured neurons (Atluri and Ryan, 2006). The slow post-stimulus endocytosis in *syp*<sup>-/-</sup> neurons was confirmed using *SV2A*-pH ( $\tau = 19.8 \pm 0.5$  s in wt,  $\tau = 30.6 \pm 1.1$  s in *syp*<sup>-/-</sup>) (Fig. 1, B and F). Direct comparison of these endocytic time constants is valid because the two genotypes have total recycling SV pools of the same size (Fig. S1, F and G). The observed

defect in the rate of endocytosis was rescued by expressing wild-type synaptophysin (wt-syp) in *syp*<sup>-/-</sup> neurons ( $\tau = 20.4 \pm 0.9$  s in *syp*<sup>-/-</sup>; wt-syp) (Fig. 1, D and F). Interestingly, when a weaker stimulation protocol was used (50 pulses, 10 Hz), the time-course of endocytosis was not significantly different between wt and *syp*<sup>-/-</sup> neurons ( $\tau = 19.3 \pm 0.4$  s in wt,  $\tau = 18.5 \pm 0.3$  s in *syp*<sup>-/-</sup>) (Fig. 1E). Interpretation of this result is provided in the Discussion section.

We performed FM 1-43 uptake experiment to test whether SV membrane recycling, in addition to trafficking of cargo proteins, was altered by loss of syp (Fig. 1G). Wt and *syp*<sup>-/-</sup> neurons were stimulated in the absence of FM 1-43 for 30 s at 10 Hz and, after a 30 s delay, were exposed to the FM dye for 3 min. Neurons were then washed for 10 min in Ca<sup>2+</sup>-free solution followed by two stimulus trains (900 pulses each at 10 Hz, 2 min rest between two trains) to drive maximal dye release from vesicles. Fluorescence changes ( $\Delta F_1$ ) were measured from images acquired before and after the 900 pulse trains. Each measurement was normalized to a subsequent control run in which FM dye was applied at the onset of stimulus without a delay; this protocol allows labeling the total pool of SVs that undergo exo- and endocytosis during and after the 30 s stimulation, yielding  $\Delta F_2$ . We hypothesized that, in wt neurons, endocytosis would be largely complete within the 30 s delay, leaving few vesicles available for FM dye uptake (Fig. 1, A and B). However, in *syp*<sup>-/-</sup> neurons, endocytosis would still be taking place during and after the 30 s delay, resulting in a larger fraction of FM dye-labeled SVs. Indeed, *syp*<sup>-/-</sup> neurons internalized more dye than wt neurons ( $0.15 \pm 0.01$  in wt,  $0.27 \pm 0.01$  in *syp*<sup>-/-</sup>), consistent with slower endocytosis observed using pHluorin (Fig. 1, H and I).

Thus, we conclude that while syp is not essential for endocytosis *per se*, it is required for kinetically efficient SV retrieval following sustained stimulation.

### Syp regulates endocytosis during neuronal activity

Recent evidence suggests that endocytosis that occurs during sustained stimulation might proceed through molecular mechanisms that are distinct from endocytosis that occurs after stimulation (Ferguson et al., 2007; Mani et al., 2007). As shown above, syp regulates vesicle retrieval following sustained neuronal activity, so we then tested whether syp functions in endocytosis during stimulation. To this end, we took advantage of the vesicular ATPase blocker, bafilomycin (Baf) that inhibits the re-acidification of SVs (Nicholson-Tomishima and Ryan, 2004). Neurons expressing SV2A-pH were stimulated at 10 Hz for 30 s in the absence of Baf, and after a 10 min rest, were stimulated again at 10 Hz for a longer time (120 s) in the presence of Baf (Fig. 2A). The difference in fluorescence intensity between the two rounds of stimulation reflects the magnitude of endocytosis that had occurred during stimulation (Fig. 2B, 'Endo') (Nicholson-Tomishima and Ryan, 2004). We derived the time-courses of vesicle retrieval during stimulation (labeled as 'endocytosis' in Fig. 2E) by calculating the difference between the upper (with Baf) and lower (without Baf) traces from each group in Fig. 2, panels B–D. Fig. 2E shows the progress of exocytosis and endocytosis during sustained stimulation for all groups. Endocytic rates were empirically estimated from the slope of the time-courses (e.g. solid line for 'wt' sample, Fig. 2E) (Nicholson-Tomishima and Ryan, 2004). The endocytic rate was decreased by ~4 fold in *syp*<sup>-/-</sup> ( $0.014$  arbitrary units (AU) s<sup>-1</sup> in wt,  $0.0035$  AU s<sup>-1</sup> in *syp*<sup>-/-</sup>), and was partially rescued by expressing wt-syp in *syp*<sup>-/-</sup> neurons ( $0.0095$  AU s<sup>-1</sup> in *syp*<sup>-/-</sup>; wt-syp) (Fig. 2, E and F). We also quantified the extent of endocytosis ('Endo') as a fraction of exocytosis ('Exo') at the end of the train ( $t = 43$  s). In *syp*<sup>-/-</sup> neurons, the extent of endocytosis (endo/exo) during sustained neuronal activity was significantly reduced as compared to wt neurons ( $0.35 \pm 0.02$  in wt,  $0.10 \pm 0.03$  in *syp*<sup>-/-</sup>,  $p < 0.001$ ); this defect was rescued by expressing wt-syp in *syp*<sup>-/-</sup> neurons ( $0.28 \pm 0.03$  in *syp*<sup>-/-</sup>; wt-syp) (Fig. 2G). Time-courses of exocytosis, estimated by fitting Baf-treated SV2A-pH traces with single exponential

functions, were identical in all groups ( $\tau = 31.0 \pm 1.2$  s in wt,  $\tau = 32.3 \pm 1.3$  s in *syp*<sup>-/-</sup>,  $\tau = 32.5 \pm 1.8$  s in *syp*<sup>-/-</sup>; wt-*syp*) (Fig. 2H). Therefore, *syp* is required for efficient SV endocytosis during, as well as following, persistent neuronal activity.

### A cytoplasmic tail of synaptophysin selectively controls endocytosis during, but not after, neuronal activity

To understand how *syp* controls the two phases of SV endocytosis, we focused on the C-terminal cytoplasmic tail which contains putative phosphorylation sites consisting of nine repeats of tyrosine-glycine-proline/glutamine (YG(P/Q)) (Sudhof et al., 1987). This tail region was reported to bind dynamin I, which is thought to mediate vesicle fission during endocytosis (Daly and Ziff, 2002; Ferguson et al., 2007). Moreover, injection of a C-terminal fragment of *syp* into the squid giant axon resulted in accelerated synaptic depression during prolonged stimulation (Daly et al., 2000; Daly and Ziff, 2002).

To address the function of the C-terminal tail of *syp*, we expressed a mutant *syp* that lacks this segment ( $\Delta$ C-*syp*, lacking amino acids 244-307 that harbor all of the nine YG(P/Q) repeats) in *syp*<sup>-/-</sup> neurons and analyzed the vesicle retrieval using SV2A-pH. Surprisingly,  $\Delta$ C-*syp* rescued the slow post-stimulus endocytosis in *syp*<sup>-/-</sup> neurons to almost the same level as the full-length protein ( $\tau = 20.9 \pm 0.7$  s in *syp*<sup>-/-</sup>;  $\Delta$ C-*syp*,  $\tau = 20.4 \pm 0.9$  s in *syp*<sup>-/-</sup>; wt-*syp*) (Fig. 3A). We then examined vesicle retrieval during stimulation using the same protocol as in Fig. 2A (Fig. 3B). As compared to wt-*syp*, the truncation mutant *syp* failed to rescue defective endocytosis during neuronal activity in terms of rate (0.0095 AU s<sup>-1</sup> in *syp*<sup>-/-</sup>; wt-*syp*, 0.0045 AU s<sup>-1</sup> in *syp*<sup>-/-</sup>;  $\Delta$ C-*syp*) (Fig. 3, C and D) and the relative magnitude of vesicle retrieval (0.28  $\pm$  0.03 in *syp*<sup>-/-</sup>; wt-*syp*, 0.14  $\pm$  0.03 in *syp*<sup>-/-</sup>;  $\Delta$ C-*syp*) (Fig. 3, B and E). These results suggest that the C-terminal domain of *syp* is selectively required for the endocytosis that occurs during, but not after, cessation of sustained synaptic transmission.

A previous study reported that the C-terminal tail is essential for internalization of *syp* in fibroblasts (Linstedt and Kelly, 1991). We tested this notion using full-length pHluorin-tagged synaptophysin (fl *sypHy*) and the mutant *sypHy* ( $\Delta$ C-*sypHy*) that lacks the same C-terminal segment (amino acids 244-307).  $\Delta$ C *sypHy* fluorescence, at the end of the 10 Hz stimulation protocol (30 s), showed a punctate distribution that was indistinguishable from full-length *sypHy*, reflecting efficient targeting to SVs (Fig. S2A). The post-stimulus endocytic time-constant of  $\Delta$ C *sypHy* ( $\tau = 18.8 \pm 0.8$  s) was not significantly different from full-length *sypHy* ( $\tau$  (Fig. S2B), indicating that the C-terminal tail of *syp* is not required for efficient internalization of *syp* following neuronal activity. Next, we tested whether trafficking of *syp*, during neuronal activity, was altered in  $\Delta$ C *sypHy* using the same protocol as in Fig. 2A. Interestingly, retrieval of  $\Delta$ C *sypHy* during neuronal activity was significantly reduced (0.31  $\pm$  0.02 for fl *sypHy*, 0.18  $\pm$  0.04 for  $\Delta$ C *sypHy*) and also became slower as compared to full-length *sypHy* (0.015 AU s<sup>-1</sup> for fl *sypHy*, 0.010 AU s<sup>-1</sup> for  $\Delta$ C *sypHy*) (Fig. S2, C and D). Thus, these results further demonstrate that different motifs within *syp* are involved in controlling the endocytosis of SV that occurs during, versus after, sustained synaptic transmission, potentially by recruiting distinct ensembles of proteins for recycling.

### *syp*<sup>-/-</sup> neurons exhibit pronounced synaptic depression and a slower recovery of the recycling vesicle pool

We investigated the physiological significance of the endocytic defects in *syp*<sup>-/-</sup> neurons by performing whole-cell voltage-clamp recordings in dissociated cortical neurons. We locally stimulated neurons by delivering electrical pulses to the cell body using a stimulating electrode and recorded evoked inhibitory post-synaptic currents (IPSCs) from the cell body

of post-synaptic partners. This method has been used to examine the dynamics of SV pools in numerous studies (Chung et al., 2010; Ferguson et al., 2007). We measured the amplitude and the kinetics of single IPSCs between wt and *syp*<sup>-/-</sup> neurons, and found that these parameters were not altered (Fig S3, A and B). Short-term plasticity, measured by paired-pulse ratio, was unaltered in *syp*<sup>-/-</sup> neurons (Fig S3, C and D). These results suggest that the absence of *syp* does not affect the neurotransmitter release probability, post-synaptic responses or short-term synaptic plasticity, consistent with a previous study (McMahon et al., 1996).

We then tested whether *syp* plays a role in maintaining the recycling SV pool during sustained neuronal activity. To this end, we stimulated neurons by delivering a train of 100 pulses at 10 Hz and monitored the depression of IPSCs during the train. The difference between wt and *syp*<sup>-/-</sup> neurons emerged after 20 stimuli and became more pronounced at later time-points; by the end of 100 stimuli, only very small IPSCs could be elicited in *syp*<sup>-/-</sup> neurons, indicating that there were few remaining vesicles ready to fuse (Fig. 4, A and B). The average steady-state amplitudes of the IPSCs, determined by averaging the last 10 responses, were as follows:  $0.171 \pm 0.04$  (wt),  $0.060 \pm 0.01$  (*syp*<sup>-/-</sup>). The pronounced synaptic depression observed in *syp*<sup>-/-</sup> neurons was completely rescued by expressing wt-*syp* (Fig. 4, C and D). In marked contrast,  $\Delta$ C-*syp* failed to rescue the enhanced depletion in *syp*<sup>-/-</sup> neurons (Fig. 4, C and D). Together with findings described above (Fig. 3), we conclude that the loss of C-terminal cytoplasmic domain leads to inefficient SV endocytosis and pronounced synaptic depression during sustained neuronal activity.

We also measured the time-course of recovery of the recycling SV pool. Neurons were stimulated at 10 Hz for 20 s to deplete vesicles, and after a brief pause, they were stimulated at 0.5 Hz to monitor re-growth of IPSCs (Fig. 4E). Amplitudes of all responses were normalized to the first response during the train. Recovery from depletion was significantly slower in *syp*<sup>-/-</sup> neurons (Fig. 4, E and F). We note that the releasable vesicle pool was not completely depleted in wt neurons even with the most intense stimulation that we were able to use without compromising cell viability (200 APs, 10 Hz in 4 mM Ca<sup>2+</sup>). Nevertheless, recovery proceeds with a much steeper slope in wt ( $\tau = 5.60$  s), as compared to *syp*<sup>-/-</sup> neurons ( $\tau = 12.8$  s) (Fig. 4F), consistent with results from pHluorin experiments shown above.

## Discussion

The data reported here firmly establish a role for *syp* in facilitating rapid and efficient SV endocytosis in mammalian central neurons. *Syp*<sup>-/-</sup> neurons exhibited defective SV endocytosis both during and after neuronal activity while exocytosis and the size of the total recycling pool of SVs were unaffected. Truncation of the C-terminal tail of *syp* led to slower endocytosis during neuronal activity, consistent with a previous study in which a tail fragment was injected into the squid giant axon (Daly et al., 2000). However, the same truncation mutant had no effect on endocytosis after neuronal activity; hence, the two endocytic processes - one during stimulation and another that is employed after stimulation - are controlled by distinct domains of *syp*.

The observed defects in SV endocytosis in *syp*<sup>-/-</sup> neurons result in functional consequences including the pronounced depletion and slower recovery of the recycling SV pool. The slow time constant of post-stimulus endocytosis might seem to be at odds with the rapid divergence of the synaptic depression time-course between wt and *syp*<sup>-/-</sup> neurons during sustained stimulation (Fig. 4, A and B). Such rapid depression observed in *syp*<sup>-/-</sup> neurons prompted us to test the possibility that rapid retrieval, or 'kiss and run' endocytosis of vesicles, is affected in the absence of *syp*. We note that whether kiss-and-run/fast retrieval

(within ~ 1 sec) is a common mode of endocytosis in hippocampal synapses remains the subject of debate (Balaji et al., 2008; Ertunc et al., 2007; Granseth et al., 2006; Zhang et al., 2009). We calculated the rate of vesicle retrieval, that occurs during stimulation, as a fraction of the total recycling pool (as determined by the maximal  $\Delta F$  values in the Baf traces) (Fig. 2, E and F). For wt neurons, only ~1.3 % of total recycling pool appears to undergo endocytosis within 1 s; this result argues against the notion that the rapid retrieval (i.e. 'kiss-and-run') predominates during sustained transmission. Hence, these results indicate that the rapid divergence of the synaptic depression time-course between wt and *syp*<sup>-/-</sup> neurons cannot be attributed to loss of putative rapid endocytosis.

An alternative explanation for the pronounced synaptic depression in *syp*<sup>-/-</sup> neurons is that *syp* might regulate another relatively rapid step, such as the clearance of vesicle release sites (Neher, 2010). Interactions between SNARE proteins on vesicular and target membranes need to be disrupted after exocytosis to allow vesicle recycling. *Syp* might facilitate this process by binding to synaptobrevin II and clearing it from active zones. The loss of *syp* might lead to a 'traffic jam' of vesicular components at release sites and thereby contribute to synaptic depression during sustained activity. However, it is not known whether the clearance of release sites is a rate-limiting step in hippocampal synapses. Finally, we note that read-outs from pHluorin imaging experiments and physiological recordings might not be directly comparable with each other due to several technical differences. These include (imaging vs electrophysiology) different methods of stimulating neurons (field stimulation vs local stimulation) and differences in temporal resolution ('s' vs 'ms'). Therefore, there are caveats regarding direct comparison of data from these two experimental approaches.

We consider the following possibilities regarding how SV endocytosis can be affected in the absence of *syp*: (1) unitary endocytic events become slower, or (2) number of SVs that can be retrieved at the same time, i.e. 'endocytic capacity' is reduced while endocytosis of individual SVs remains unaffected (Balaji et al., 2008). Since we only measured the macroscopic time-courses of vesicle retrieval, we cannot completely distinguish between these two possibilities. Nevertheless, the finding that compensatory vesicle retrieval in *syp*<sup>-/-</sup> became slower only after 300 stimuli argues the first scenario. Indeed, the rate of unitary endocytic events is reported to be largely invariant (Balaji et al., 2008). Therefore, we propose that the role of *syp* is to maintain endocytic capacity in synapses. At the molecular level, *syp* may recruit or promote the assembly of endocytic components in order to maintain the number of available 'endocytic machines' during and after sustained neuronal activity.

It will be of interest to determine whether SV endocytosis is further affected in *syp* and synaptogyrin double knockout mice with impaired long-term potentiation, a neural substrate for learning and memory (Janz et al., 1999). Future studies will also focus on the molecular mechanisms through which *syp* interacts with binding partners – e.g. synaptobrevin II, dynamin I, and adaptor protein-I - to control vesicle recycling (Daly and Ziff, 2002; Edelman et al., 1995; Glyvuk et al., 2010; Horikawa et al., 2002). Given that *syb* II plays a role in vesicle endocytosis and that *syp* promotes vesicular localization of *syb* II, it is tempting to speculate that the function of *syp* in efficient SV endocytosis might involve a physical interaction with *syb* II (Deak et al., 2004; Hosoi et al., 2009; Wienisch and Klingauf, 2006).

## Experimental Procedures

### Molecular Biology

Syt1-pH and sypHy constructs were kindly provided by T.A Ryan (New York, NY) and L. Lagnado (Cambridge, UK), respectively. SV2A-pH is described in Supplemental Experimental Procedures

### Neuronal Cultures and Viruses

A syp knock out mouse line was kindly provided by R. Leube (Mainz, Germany) (Eshkind and Leube, 1995). The mouse line was maintained as heterozygous breeding pairs. Primary hippocampal cultures were prepared as described previously in accordance with the guidelines of the National Institutes of Health, as approved by the Animal Care and Use Committee of the University of Wisconsin–Madison (Liu et al., 2009). Viruses were generated in human embryonic kidney 293T cells as previously described (Dong et al., 2006). See Supplemental Experimental Procedures for details.

### Live-cell Imaging

Neurons were continuously perfused with bath solution (140 mM NaCl, 5 mM KCl, 2 mM CaCl<sub>2</sub>, 2 mM MgCl<sub>2</sub>, 10 mM HEPES, 10 mM Glucose, 50 μM D-AP5, 10 μM CNQX adjusted to 310 mOsm with glucose, pH 7.4) at room temperature during imaging. During resting or washing steps, the 2 mM Ca<sup>2+</sup> was replaced with 2 mM Mg<sup>2+</sup>. For field-stimulation, 1 ms constant voltage pulses (70 V) were delivered digitally using ClampEX 10.0 via two parallel platinum wires spaced by 10 mm in the imaging chamber (Warner Instruments). Time-lapse images taken at 1 s intervals were obtained on an inverted microscope (Nikon TE300) with a 100× oil objective under illumination with a xenon light source (Lambda DG4). Fluorescence changes at individual boutons were detected using a Cascade 512II EMCCD camera (Roper Scientific) with 2×2 binning; data were collected and analyzed off-line using MetaMorph 6.0 software. See Supplemental Experimental Procedures for details.

### Electrophysiology

Whole-cell voltage-clamp recordings of evoked IPSCs were performed using an AxoPatch 200B amplifier (Molecular Devices) driven by pClamp 10. The internal pipette solution contained the following (in mM): 135 CsCl<sub>2</sub>, 1 EGTA, 10 HEPES, 1 NaGTP, 4 QX-314 (pH 7.4). Cells were continuously perfused with extracellular fluid (ECF): 140 mM NaCl, 5 mM KCl, 3 mM CaCl<sub>2</sub>, 2 mM MgCl<sub>2</sub>, 10 mM HEPES, 10 mM Glucose, 50 μM D-AP5, 10 μM CNQX, adjusted to 310 mOsm with glucose, pH 7.4. Recordings with a series resistance significantly larger than 20 MΩ were discarded. When 4 mM Ca<sup>2+</sup> was used as in Fig. 4E, [Mg<sup>2+</sup>] was lowered to 1 mM. Action potentials were evoked by stimulating presynaptic neurons with a theta stimulating electrode with a voltage of 20–30 V for 1 ms. Data were sampled at 10 kHz, and filtered at 2 kHz.

### Supplementary Material

Refer to Web version on PubMed Central for supplementary material.

### Acknowledgments

We thank M. Jackson and X. Lou for their comments on this manuscript. We also thank M. Dong and M. Dunning for help with cDNA constructs used to carry out this work. This study was supported by a grant from the NIH (MH061876). S.E.K was supported by Epilepsy Foundation predoctoral fellowship. E.R.C is an Investigator of the Howard Hughes Medical Institute.

## References

- Arthur CP, Stowell MH. Structure of synaptophysin: a hexameric MARVEL-domain channel protein. *Structure*. 2007; 15:707–714. [PubMed: 17562317]
- Atluri PP, Ryan TA. The kinetics of synaptic vesicle reacidification at hippocampal nerve terminals. *J Neurosci*. 2006; 26:2313–2320. [PubMed: 16495458]
- Balaji J, Armbruster M, Ryan TA. Calcium control of endocytic capacity at a CNS synapse. *J Neurosci*. 2008; 28:6742–6749. [PubMed: 18579748]
- Cameron PL, Sudhof TC, Jahn R, De Camilli P. Colocalization of synaptophysin with transferrin receptors: implications for synaptic vesicle biogenesis. *J Cell Biol*. 1991; 115:151–164. [PubMed: 1918133]
- Chung C, Barylko B, Leitz J, Liu X, Kavalali ET. Acute dynamin inhibition dissects synaptic vesicle recycling pathways that drive spontaneous and evoked neurotransmission. *J Neurosci*. 2010; 30:1363–1376. [PubMed: 20107062]
- Daly C, Sugimori M, Moreira JE, Ziff EB, Llinas R. Synaptophysin regulates clathrin-independent endocytosis of synaptic vesicles. *Proc Natl Acad Sci U S A*. 2000; 97:6120–6125. [PubMed: 10823955]
- Daly C, Ziff EB. Ca<sup>2+</sup>-dependent formation of a dynamin-synaptophysin complex: potential role in synaptic vesicle endocytosis. *J Biol Chem*. 2002; 277:9010–9015. [PubMed: 11779869]
- Deak F, Schoch S, Liu X, Sudhof TC, Kavalali ET. Synaptobrevin is essential for fast synaptic-vesicle endocytosis. *Nat Cell Biol*. 2004; 6:1102–1108. [PubMed: 15475946]
- Dong M, Yeh F, Tepp WH, Dean C, Johnson EA, Janz R, Chapman ER. SV2 is the protein receptor for botulinum neurotoxin A. *Science*. 2006; 312:592–596. [PubMed: 16543415]
- Edelmann L, Hanson PI, Chapman ER, Jahn R. Synaptobrevin binding to synaptophysin: a potential mechanism for controlling the exocytotic fusion machine. *Embo J*. 1995; 14:224–231. [PubMed: 7835333]
- Ertunc M, Sara Y, Chung C, Atasoy D, Virmani T, Kavalali ET. Fast synaptic vesicle reuse slows the rate of synaptic depression in the CA1 region of hippocampus. *J Neurosci*. 2007; 27:341–354. [PubMed: 17215395]
- Eshkind LG, Leube RE. Mice lacking synaptophysin reproduce and form typical synaptic vesicles. *Cell Tissue Res*. 1995; 282:423–433. [PubMed: 8581936]
- Evans GJ, Cousin MA. Tyrosine phosphorylation of synaptophysin in synaptic vesicle recycling. *Biochem Soc Trans*. 2005; 33:1350–1353. [PubMed: 16246116]
- Ferguson SM, Brasnjo G, Hayashi M, Wolfel M, Collesi C, Giovedi S, Raimondi A, Gong LW, Ariel P, Paradise S, et al. A selective activity-dependent requirement for dynamin 1 in synaptic vesicle endocytosis. *Science*. 2007; 316:570–574. [PubMed: 17463283]
- Fernandez-Alfonso T, Kwan R, Ryan TA. Synaptic vesicles interchange their membrane proteins with a large surface reservoir during recycling. *Neuron*. 2006; 51:179–186. [PubMed: 16846853]
- Glyvuk N, Tsytsyura Y, Geumann C, D’Hooge R, Huve J, Kratzke M, Baltes J, Boening D, Klingauf J, Schu P. AP-1/sigma1B-adaptin mediates endosomal synaptic vesicle recycling, learning and memory. *Embo J*. 2010; 29:1318–1330. [PubMed: 20203623]
- Granseth B, Odermatt B, Royle SJ, Lagnado L. Clathrin-mediated endocytosis is the dominant mechanism of vesicle retrieval at hippocampal synapses. *Neuron*. 2006; 51:773–786. [PubMed: 16982422]
- Horikawa HP, Kneussel M, El Far O, Betz H. Interaction of synaptophysin with the AP-1 adaptor protein gamma-adaptin. *Mol Cell Neurosci*. 2002; 21:454–462. [PubMed: 12498786]
- Hosoi N, Holt M, Sakaba T. Calcium dependence of exo- and endocytotic coupling at a glutamatergic synapse. *Neuron*. 2009; 63:216–229. [PubMed: 19640480]
- Jahn R, Schiebler W, Ouimet C, Greengard P. A 38,000-dalton membrane protein (p38) present in synaptic vesicles. *Proc Natl Acad Sci U S A*. 1985; 82:4137–4141. [PubMed: 3923488]
- Janz R, Sudhof TC, Hammer RE, Unni V, Siegelbaum SA, Bolshakov VY. Essential roles in synaptic plasticity for synaptogyrin I and synaptophysin I. *Neuron*. 1999; 24:687–700. [PubMed: 10595519]



- Leube RE. The topogenic fate of the polytopic transmembrane proteins, synaptophysin and connexin, is determined by their membrane-spanning domains. *J Cell Sci.* 1995; 108(Pt 3):883–894. [PubMed: 7622617]
- Leube RE, Wiedenmann B, Franke WW. Topogenesis and sorting of synaptophysin: synthesis of a synaptic vesicle protein from a gene transfected into nonneuroendocrine cells. *Cell.* 1989; 59:433–446. [PubMed: 2478297]
- Linstedt AD, Kelly RB. Endocytosis of the synaptic vesicle protein, synaptophysin, requires the COOH-terminal tail. *J Physiol (Paris).* 1991; 85:90–96. [PubMed: 1757893]
- Liu H, Dean C, Arthur CP, Dong M, Chapman ER. Autapses and networks of hippocampal neurons exhibit distinct synaptic transmission phenotypes in the absence of synaptotagmin I. *J Neurosci.* 2009; 29:7395–7403. [PubMed: 19515907]
- Mani M, Lee SY, Lucast L, Cremona O, Di Paolo G, De Camilli P, Ryan TA. The dual phosphatase activity of synaptojanin1 is required for both efficient synaptic vesicle endocytosis and reavailability at nerve terminals. *Neuron.* 2007; 56:1004–1018. [PubMed: 18093523]
- McMahon HT, Bolshakov VY, Janz R, Hammer RE, Siegelbaum SA, Sudhof TC. Synaptophysin, a major synaptic vesicle protein, is not essential for neurotransmitter release. *Proc Natl Acad Sci U S A.* 1996; 93:4760–4764. [PubMed: 8643476]
- Miesenbock G, De Angelis DA, Rothman JE. Visualizing secretion and synaptic transmission with pH-sensitive green fluorescent proteins. *Nature.* 1998; 394:192–195. [PubMed: 9671304]
- Navone F, Jahn R, Di Gioia G, Stukenbrok H, Greengard P, De Camilli P. Protein p38: an integral membrane protein specific for small vesicles of neurons and neuroendocrine cells. *J Cell Biol.* 1986; 103:2511–2527. [PubMed: 3097029]
- Neher E. What is rate-limiting during sustained synaptic activity: vesicle supply or the availability of release sites. *Frontiers in Synaptic Neuroscience.* 2010; 2:1–6. [PubMed: 21423487]
- Nicholson-Tomishima K, Ryan TA. Kinetic efficiency of endocytosis at mammalian CNS synapses requires synaptotagmin I. *Proc Natl Acad Sci U S A.* 2004; 101:16648–16652. [PubMed: 15492212]
- Pang DT, Wang JK, Valtorta F, Benfenati F, Greengard P. Protein tyrosine phosphorylation in synaptic vesicles. *Proc Natl Acad Sci U S A.* 1988; 85:762–766. [PubMed: 3124110]
- Sankaranarayanan S, Ryan TA. Real-time measurements of vesicle-SNARE recycling in synapses of the central nervous system. *Nat Cell Biol.* 2000; 2:197–204. [PubMed: 10783237]
- Schmitt U, Tanimoto N, Seeliger M, Schaeffel F, Leube RE. Detection of behavioral alterations and learning deficits in mice lacking synaptophysin. *Neuroscience.* 2009; 162:234–243. [PubMed: 19393300]
- Spiwoks-Becker I, Vollrath L, Seeliger MW, Jaissle G, Eshkind LG, Leube RE. Synaptic vesicle alterations in rod photoreceptors of synaptophysin-deficient mice. *Neuroscience.* 2001; 107:127–142. [PubMed: 11744253]
- Sudhof TC, Lottspeich F, Greengard P, Mehl E, Jahn R. A synaptic vesicle protein with a novel cytoplasmic domain and four transmembrane regions. *Science.* 1987; 238:1142–1144. [PubMed: 3120313]
- Takamori S, Holt M, Stenius K, Lemke EA, Grønborg M, Riedel D, Urlaub H, Schenck S, Brügger B, Ringler P, et al. Molecular anatomy of a trafficking organelle. *Cell.* 2006; 127:831–846. [PubMed: 17110340]
- Tarpey PS, Smith R, Pleasance E, Whibley A, Edkins S, Hardy C, O’Meara S, Latimer C, Dicks E, Menzies A, et al. A systematic, large-scale resequencing screen of X-chromosome coding exons in mental retardation. *Nat Genet.* 2009; 41:535–543. [PubMed: 19377476]
- Tarsa L, Goda Y. Synaptophysin regulates activity-dependent synapse formation in cultured hippocampal neurons. *Proc Natl Acad Sci U S A.* 2002; 99:1012–1016. [PubMed: 11792847]
- Thiele C, Hannah MJ, Fahrenholz F, Huttner WB. Cholesterol binds to synaptophysin and is required for biogenesis of synaptic vesicles. *Nat Cell Biol.* 2000; 2:42–49. [PubMed: 10620806]
- Thomas L, Hartung K, Langosch D, Rehm H, Bamberg E, Franke WW, Betz H. Identification of synaptophysin as a hexameric channel protein of the synaptic vesicle membrane. *Science.* 1988; 242:1050–1053. [PubMed: 2461586]

- Wiedenmann B, Franke WW. Identification and localization of synaptophysin, an integral membrane glycoprotein of Mr 38,000 characteristic of presynaptic vesicles. *Cell*. 1985; 41:1017–1028. [PubMed: 3924408]
- Wienisch M, Klingauf J. Vesicular proteins exocytosed and subsequently retrieved by compensatory endocytosis are nonidentical. *Nat Neurosci*. 2006; 9:1019–1027. [PubMed: 16845386]
- Zhang Q, Li Y, Tsien RW. The dynamic control of kiss-and-run and vesicular reuse probed with single nanoparticles. *Science*. 2009; 323:1448–1453. [PubMed: 19213879]

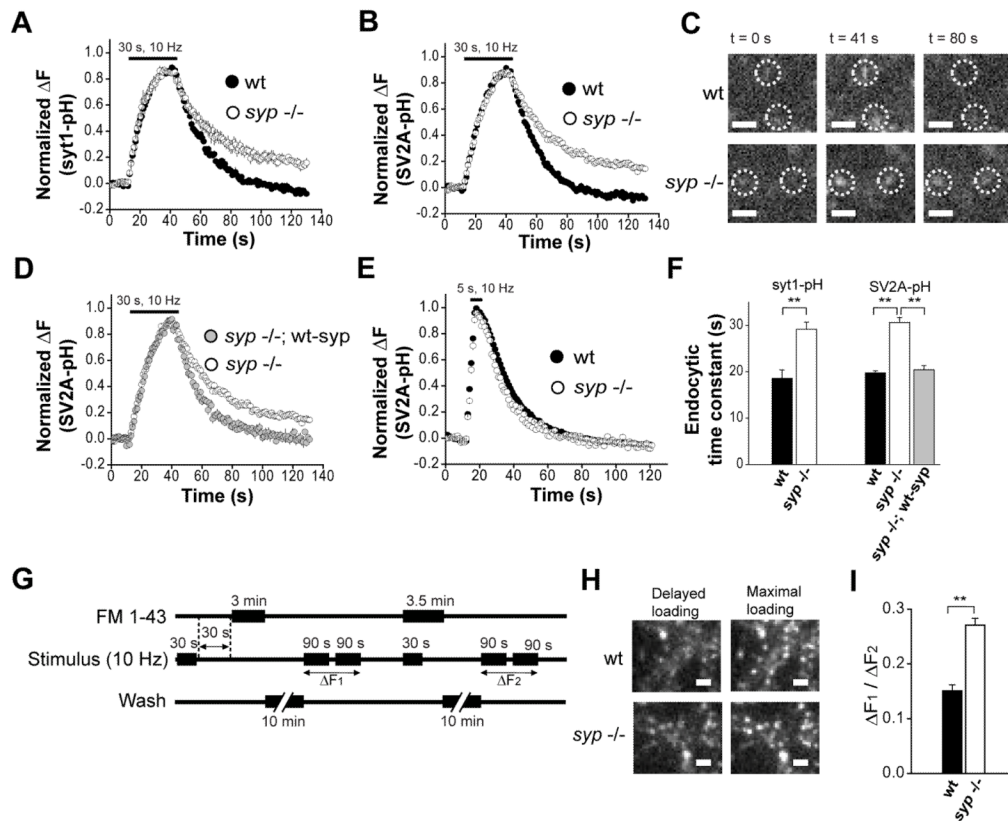


**Figure 1. Syp regulates endocytosis of SVs following cessation of persistent neuronal activity** (A) Average traces of wild-type (black) and *syp*<sup>-/-</sup> (white) neurons expressing synaptotagmin 1-pHluorin (syt1-pH) in response to 300 stimuli at 10 Hz. Average from 3 coverslips, 20 boutons each. (B) Average traces of wild-type (black) and *syp*<sup>-/-</sup> (white) neurons expressing SV2A-pHluorin (SV2A-pH) in response to 300 stimuli at 10 Hz. Average from 6 coverslips, 30 boutons each. (C) Fluorescence images showing pre-synaptic boutons expressing SV2A-pH in wt and *syp*<sup>-/-</sup> neurons, before stimulation (t = 0) and following cessation of stimulation (t = 41 s or 80 s) at 10 Hz for 30 s. 't' indicates a time-point on the horizontal axis of the plot shown in (B). Scale bars are 2  $\mu$ m. (D) Average SV2A-pH traces of *syp*<sup>-/-</sup> (white, 6 coverslips, 30 boutons each) and wt-syp rescue (grey, 5 coverslips, 30 boutons each) neurons in response to 300 stimuli at 10 Hz. (E) Average SV2A-pH traces of wild-type (black) and *syp*<sup>-/-</sup> (white) neurons in response to 50 stimuli at 10 Hz. Average from 4 coverslips, 40 boutons each. (F) Comparison of average post-stimulus endocytic time constants between wild-type, *syp*<sup>-/-</sup> and wt-syp rescue neurons. All  $\Delta F$  values were normalized to the maximal fluorescence intensity change. The decay phases of  $\Delta F$  traces from syt1-pH or SV2A-pH were fitted with single exponential functions before normalization, and the time constants were calculated from the fits. (G) Protocol for FM 1-43 pulse-chase experiments. Neurons were stimulated at 10 Hz for 30 s. After a short delay (30 s), neurons were exposed to FM 1-43 for 3 min and then washed in  $Ca^{2+}$  solution for 10 min. Two trains of 900 pulses (10 Hz) were delivered to evoke unloading of FM 1-43. After a 10 min rest, neurons were stimulated at 10 Hz for 30 s in the presence of FM 1-43. This was followed by washing and unloading in the same manner as the first round. (H) Fluorescence images showing pre-synaptic boutons expressing FM 1-43 in wt and *syp*<sup>-/-</sup> neurons, before stimulation (Delayed loading) and following cessation of stimulation (Maximal loading) at 10 Hz for 30 s. Scale bars are 2  $\mu$ m. (I) Comparison of average post-stimulus fluorescence changes between wild-type, *syp*<sup>-/-</sup> and wt-syp rescue neurons. All  $\Delta F$  values were normalized to the maximal fluorescence intensity change. The ratio of fluorescence changes was calculated from the fits.

(H) Sample images showing boutons labeled with FM 1-43 during the delayed loading (Left panels) and the maximal loading (Right panels). Scale bars are 1.5  $\mu\text{m}$ .

(I) Average  $\Delta F_1/\Delta F_2$  ratio of wt and *syp*<sup>-/-</sup> neurons. Average from 4 coverslips, 40 boutons each. All error bars are SEM. \*\*,  $p < 0.001$  (two-tailed, unpaired *t*-test throughout).

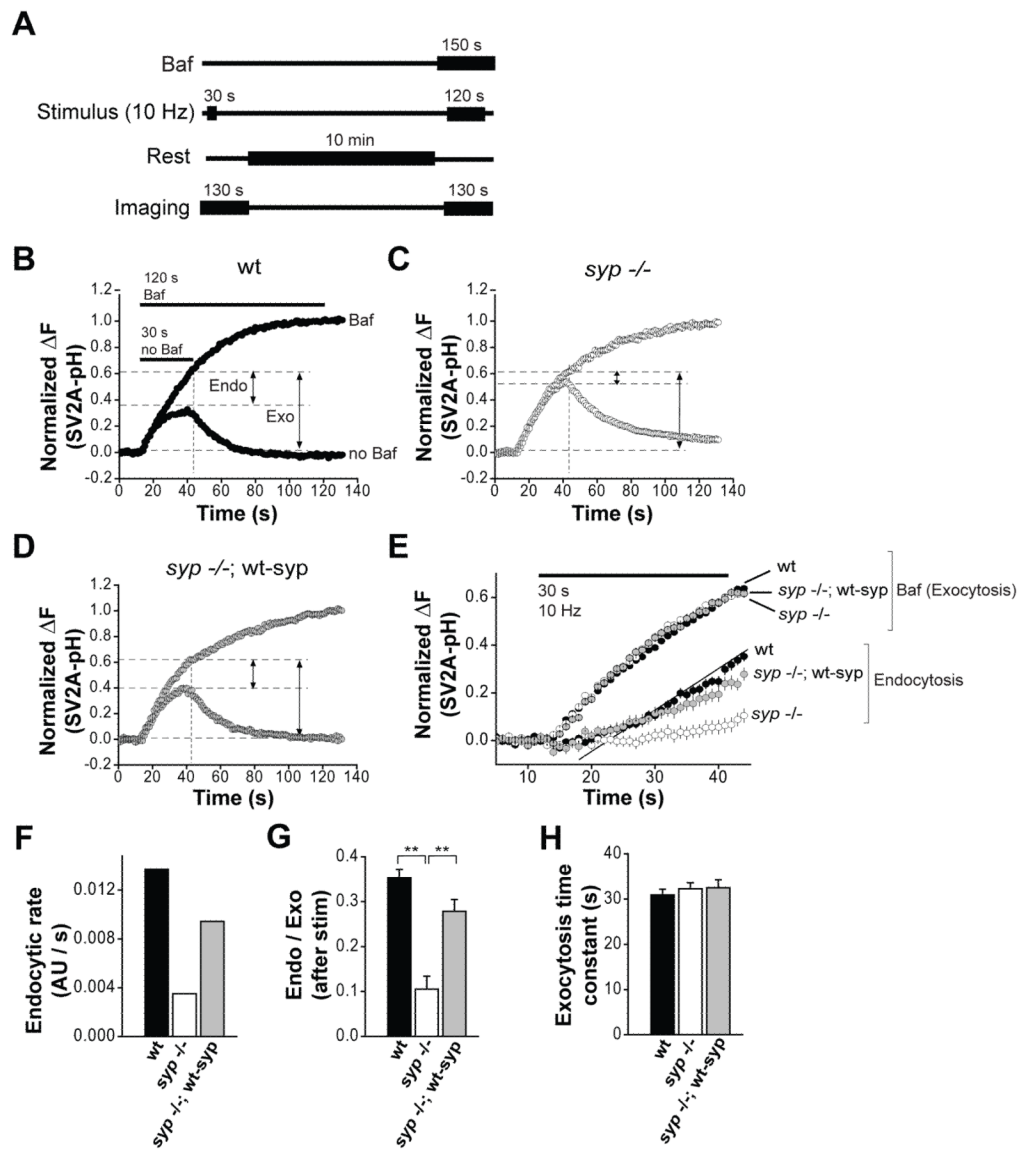


**Figure 2. Endocytosis during sustained synaptic transmission is reduced in *syp*<sup>-/-</sup> neurons**

(A) Protocol for measuring time-course and extent of endocytosis during neuronal activity using bafilomycin (Baf) to prevent vesicle re-acidification. Neurons expressing SV2A-pH were stimulated at 10 Hz for 30 s in the absence of Baf. After a 10 min rest, neurons were stimulated at 10 Hz for 120 s in the presence of Baf. Images were acquired during each phase of stimulation.

(B) Average SV2A-pH traces from wt neurons in response to 300 stimuli at 10 Hz. Traces represent averages from 6 coverslips, 30 boutons each. Values were normalized to the maximum fluorescence change at the end of 1200 stimuli in presence of Baf. The short and long arrows (also in (C) and (D)) indicate the extent of endocytosis and exocytosis at the end of the 300 stimuli (vertical dashed line) at 10 Hz respectively.

(C) The same experiment was repeated in *syp*<sup>-/-</sup> neurons (6 coverslips, 30 boutons each)

(D) The same experiment was repeated in wt-syp rescue samples (5 coverslips, 30 boutons each).

(E) Time-courses of exocytosis (Baf) and endocytosis for wt, *syp*<sup>-/-</sup> and wt-*syp* rescue neurons during stimulation (30 s, 10 Hz). Each endocytosis time-course was calculated by subtracting the SV2A-pH trace that was acquired in the absence of Baf, from the ‘Baf’ trace in panels (B–D). Endocytosis traces were fitted with linear functions (solid line shown as an example for ‘wt’). Endocytic rates were determined empirically by calculating slope of the fitted lines.

(F) Endocytic rates (in arbitrary units per second (AU/s)) as determined in (E).

(G) Average magnitude of endocytosis as a fraction of exocytosis after delivery of 300 pulses.

(H) Average exocytic time constants estimated by fitting the rising phase of Baf traces in panels (B–D) with single exponential functions.

All error bars are SEM. \*\*,  $p < 0.001$ .

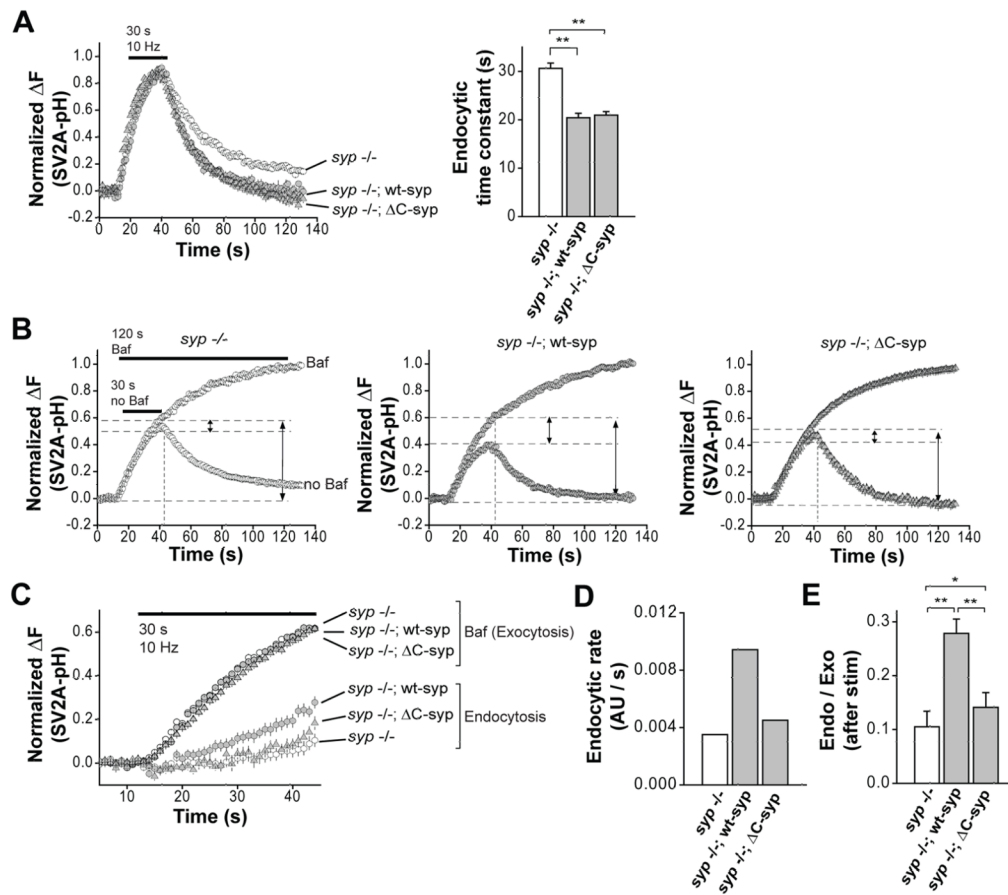


**Figure 3. The C-terminal cytoplasmic tail of synaptophysin regulates endocytosis during persistent neuronal activity, but is not important for post-stimulus endocytosis**

(A) (Left) Average SV2A-pH traces of *syp*<sup>-/-</sup> (white, 6 coverslips, 30 boutons each), wt-syp rescue (black, 5 coverslips, 30 boutons each) and  $\Delta C$ -syp neurons (grey, 5 coverslips, 30 boutons each) in response to 300 stimuli at 10 Hz. (Right) Comparison of average post-stimulus endocytic time constants between *syp*<sup>-/-</sup>, wt-syp rescue and  $\Delta C$ -syp neurons.

(B) Endocytosis during neuronal activity was assayed using the same protocol as shown in Fig. 2(A). Each trace is an average of the same number of samples as in (A). Time-courses of exocytosis (Baf) and endocytosis for *syp*<sup>-/-</sup> (Left), wt-syp rescue (Middle) and  $\Delta C$ -syp neurons (Right) during the 30 s stimulation protocol.

(C) Time-courses of exocytosis (Baf) and endocytosis for *syp*<sup>-/-</sup>, wt-syp rescue  $\Delta C$ -syp neurons during the 30 s stimulation at 10 Hz. Each endocytosis time-course was calculated by subtracting the SV2A-pH trace that was acquired in the absence of Baf, from the ‘Baf’ trace in each of the three panels in (B). Endocytic rates were determined by fitting the slope with linear functions as in Fig. 2(E).

(D) Endocytic rates (in AU/s) as determined in (C).

(E) Average magnitude of endocytosis as a fraction of exocytosis after delivery of 300 stimuli.

All error bars are SEM. \*,  $p < 0.05$ , \*\*,  $p < 0.001$ .

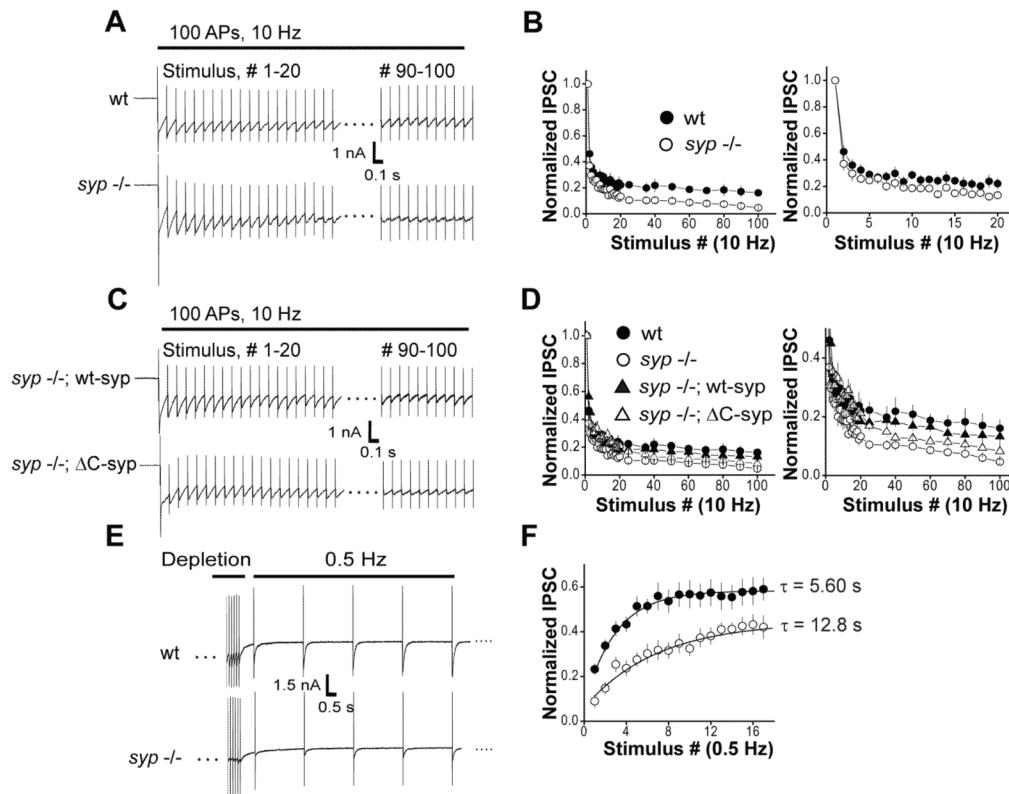


**Figure 4. Time courses of synaptic depression and recovery in *syp*<sup>-/-</sup> neurons**

(A) Representative traces of evoked inhibitory post-synaptic currents (IPSCs) in wt (top) and *syp*<sup>-/-</sup> (bottom) during 100 stimuli at 10 Hz in 3 mM Ca<sup>2+</sup>.

(B) (Top) Normalized IPSC amplitudes in wt (black) and *syp*<sup>-/-</sup> (white) neurons during sustained 10 Hz stimulation. Values are averages from 7 wt and 7 *syp*<sup>-/-</sup> neurons.

Amplitude values were normalized to the first response in the train. (Bottom) Averages of the first twenty responses during 10 Hz stimulation are shown for clarity.

(C) Representative traces of IPSCs in wt-syp (Top) and ΔC-syp (Bottom) neurons during 100 stimuli at 10 Hz in 3 mM Ca<sup>2+</sup>.

(D) Normalized IPSC amplitudes from wt-syp rescue (grey) and ΔC-syp neurons (grey triangle) are overlaid with wt and *syp*<sup>-/-</sup> data from (B). Values are averages from 8 wt-syp and 6 ΔC-syp samples.

(E) Representative traces of IPSCs from vesicle pool recovery experiments. Neurons were subjected to two separate phases of stimulation: 200 stimuli at 10 Hz in 4 mM Ca<sup>2+</sup> for maximal depletion of the recycling SV pool, and then a recovery phase with mild stimulation at 0.5 Hz.

(F) Normalized IPSC amplitudes from wt (black) and *syp*<sup>-/-</sup> (white) neurons during the recovery phase. Amplitude values were normalized to the first response in the depletion phase and fitted with single exponential functions. Values are averages from 8 wt and 8 *syp*<sup>-/-</sup> neurons.

All error bars are SEM.